

A Markov Chain Monte Carlo Study on Dark Matter Property Related to the Cosmic e^\pm Excesses

Jie Liu^a, Qiang Yuan^b, Xiaojun Bi^b, Hong Li^{a,c}, and Xinmin Zhang^{a,c}

^a*Theoretical Physics Division, Institute of High Energy Physics,
Chinese Academy of Science, P.O.Box 918-4, Beijing 100049, P.R.China*

^b*Key Laboratory of Particle Astrophysics,
Institute of High Energy Physics, Chinese Academy of Science,
P.O.Box 918-3, Beijing 100049, P.R.China and*

^c*Theoretical Physics Center for Science Facilities (TPCSF),
Chinese Academy of Science, P.R.China*

In this paper we develop a Markov Chain Monte Carlo code to study the dark matter properties in frameworks to interpret the recent observations of cosmic ray electron/positron excesses. We assume that the dark matter particles couple dominantly to leptons and consider two cases, annihilating or decaying into lepton pairs, respectively. The constraint on the central density profile from H.E.S.S. observation of diffuse γ -rays around the Galactic center is also included in the Markov Chain Monte Carlo code self-consistently. In the numerical study, we have considered two cases of the background: fixed e^+e^- background and the relaxed one. Two data sets of electrons/positrons, i.e. PAMELA+ATIC (Data set I) and PAMELA+Fermi-LAT+H.E.S.S. (Data set II), are fitted independently, considering the current inconsistency between the observational data. We find that for the Data set I, dark matter with $m_\chi \approx 0.70$ TeV for annihilation (or 1.4 TeV for decay) and a non-negligible branching ratio to e^+e^- channel is favored; while for the Data set II, $m_\chi \approx 2.2$ TeV for annihilation (or 4.5 TeV for decay) and the combination of $\mu^+\mu^-$ and $\tau^+\tau^-$ final states can best fit the data. We also show that the background of electrons and positrons actually will significantly affect the branching ratios. The H.E.S.S. observation of γ -rays in Galactic center ridge puts a strong constraint on the central density profile of the dark matter halo for the annihilation dark matter scenario. In this case the NFW profile which is regarded as the typical predication from the cold dark matter scenario, is excluded with a high significance ($> 3\sigma$). For the decaying

dark matter scenario, the constraint is much weaker.

PACS numbers: 98.80.Es; 98.80.Cq

I. INTRODUCTION

The recent reported results on the abnormal excesses of cosmic ray (CR) positron fraction by PAMELA [1] and the spectra of electrons¹ by ATIC [2], PPB-BETS [3], H.E.S.S. [4, 5] and Fermi-LAT [6] have invoked extensive discussions on the possible existence of dark matter (DM) signals (for a recent review, see e.g., [7, 8]). Meanwhile, the ratio of antiproton to proton measured by PAMELA [9] is well consistent with the astrophysical expectation from interactions between CR nuclei and interstellar medium (ISM) [10]. It indicates that if the DM contributes to the electron/positron excesses, it should dominantly annihilate or decay into leptons instead of gauge bosons or quarks [11, 12]. Although the observational data of the electron spectra from ATIC and Fermi-LAT/H.E.S.S. are not fully consistent, it has been shown in literature that the DM models with annihilation or decay modes directly to leptons can give good description to the observational data, given proper mass of DM particle and flavors of the final state particles (e.g., [13–16]). Specifically, the ATIC data favor a e^+e^- channel to describe the bump and fast drop for energy ~ 600 GeV [2, 17]. While for Fermi-LAT and H.E.S.S. data, a softer electron/positron spectrum from the decay of $\mu^+\mu^-$ or $\tau^+\tau^-$ final states can better reproduce the smooth behavior [15, 16].

However, for the numerical studies of fitting to the data in the literature so far one usually takes some specific parameters for a given model, then fits to the data for illustrations of how the model works instead of performing a global analysis. Therefore bias exists in the conclusions drawn from this kind of studies. A global fit to the observational data thus will be very useful to extract the model-independent implication from the data and to explore the correlations among different parameters. In this work we employ a Markov Chain Monte Carlo (MCMC) technique [18–20] to globally fit the parameters of the DM scenario to the experimental data on the electron/positron spectrum observed. The constraint from the diffuse γ -ray emission around the Galactic center (GC), known as GC ridge, by H.E.S.S.

¹ When we mention about experimental data of electron spectra, it actually means the total spectra of electrons and positrons.

[21] is also included in the MCMC program. Based on the global fitting results, we can then further investigate the possible implication on the models of both on the particle physical side and also the astrophysical side of DM, in a manner of self-consistency.

Another issue which is not seriously taken into account in previous studies is the influence of electron/positron background on the DM models. The global fit method makes it possible to include the uncertainties of the background contribution. This point is also discussed in this work.

The paper is organized as follows. In Sec. II we introduce the production mechanism of the electrons and positrons generated from DM annihilation or decay, and their propagation effect in the Milky Way (MW). In Sec. III we describe the accompanied γ -rays which are served as a cross check of the self-consistency of the model configuration. The MCMC fitting procedure and results are given in Sec. IV. Finally, Sec. V is the summary.

II. PRODUCTION AND PROPAGATION OF THE COSMIC e^\pm

Due to the constraints from \bar{p}/p by PAMELA, the DM is thought to be dominantly coupled with leptons [11, 12]. Since in this work we mainly focus on the methodology of using MCMC to globally fit the observational data, we will limit our discussion in the cases that DM annihilates or decays to lepton pairs directly². The production rate of electrons (positrons) can be written as

$$q_e(\mathbf{r}, E) = \frac{\langle\sigma v\rangle}{2m_\chi^2} \left. \frac{dN}{dE} \right|_i \rho^2(\mathbf{r}), \quad (1)$$

for DM annihilation, or

$$q_e(\mathbf{r}, E) = \frac{1}{m_\chi \tau} \left. \frac{dN}{dE} \right|_i \rho(\mathbf{r}), \quad (2)$$

for DM decay, where m_χ is the mass of DM particle, $\langle\sigma v\rangle$ or τ are the annihilation cross section or decay age of DM respectively, $\left. \frac{dN}{dE} \right|_i$ is the electron yield spectrum for one annihilation or decay with $i = e, \mu, \tau$, and $\rho(\mathbf{r})$ is DM spatial density in the MW halo. The density profile of the MW halo is taken as the form

$$\rho(r) = \frac{\rho_s}{(r/r_s)^\gamma (1 + r/r_s)^{3-\gamma}}, \quad (3)$$

² A more general discussion including the quarks or gauge bosons in the final states will be a straightforward extension of the current study and will be present in a future publication.

where γ represents the central cusp slope of the density profile, r_s and ρ_s are scale radius and density respectively. For the MW DM halo, we adopt the total mass to be $M_{\text{MW}} \approx 10^{12} M_\odot$ [22] and the concentration parameter to be $c_{\text{MW}} \approx 13.5$ [23]. Then we have $r_s = r_{\text{MW}}/c_{\text{MW}}(2 - \gamma)$ where $r_{\text{MW}} \approx 260$ kpc is the virial radius of MW halo. Then ρ_s can be derived by requiring $M_{\text{MW}} = \int \rho dV$. The local density ρ_\odot in this process is checked to be within 0.27 to 0.25 GeV cm⁻³ for γ varying from 0 to 1.5.

After the production from DM annihilation or decay, the electrons and positrons will propagate diffusively in the MW due to the scattering with the random magnetic field. Besides the diffusion, the dominant process of electron propagation is the energy loss from synchrotron radiation in Galactic magnetic field and the inverse Compton (IC) scatterings in the interstellar radiation field (ISRF). There may also be global convection driven by stellar wind and reacceleration by random interstellar shock, however, as shown in Ref. [24], these effects can be safely neglected for electron energy $\gtrsim 10$ GeV. The propagation equation is

$$-D\nabla^2 N(\mathbf{r}, E) + \frac{\partial}{\partial E} \left[\frac{dE}{dt} N(\mathbf{r}, E) \right] = q(\mathbf{r}, E), \quad (4)$$

where $D(E) = \beta D_0 \mathcal{R}^\delta$ ($\mathcal{R} = pc/Ze$ is the rigidity) is the diffusion coefficient, $dE/dt = -\epsilon^2/\tau_E$ with $\epsilon = E/1$ GeV and $\tau_E \approx 10^{16}$ s, is the energy loss rate for typical values of the Galactic magnetic field and ISRF, $q(\mathbf{r}, E)$ is the source function of e^\pm as given in Eqs. (1) and (2), and $N(\mathbf{r}, E)$ is the propagated e^\pm spectrum.

The propagator for a point source located at (r, z) from the solar location with monochromatic injection energy E_S can be written as [25, 26]

$$\mathcal{G}_\odot(r, z, E \leftarrow E_S) = \frac{\tau_E}{E\epsilon} \times \hat{\mathcal{G}}_\odot(r, z, \hat{\tau}), \quad (5)$$

in which we define a pseudo time $\hat{\tau}$ as

$$\hat{\tau} = \tau_E \frac{\epsilon^{\delta-1} - \epsilon_S^{\delta-1}}{1 - \delta}. \quad (6)$$

$\hat{\mathcal{G}}_\odot(r, z, \hat{\tau})$ is the Green's function for the re-arranged diffusion equation with respect to the pseudo time $\hat{\tau}$

$$\hat{\mathcal{G}}_\odot(r, z, \hat{\tau}) = \frac{\theta(\hat{\tau})}{4\pi D_0 \hat{\tau}} \exp\left(-\frac{r^2}{4D_0 \hat{\tau}}\right) \times \mathcal{G}^{1D}(z, \hat{\tau}). \quad (7)$$

The effect of boundaries along $z = \pm L$ appears in \mathcal{G}^{1D} only. Following Ref. [25] we use two distinct regimes to approach \mathcal{G}^{1D} :

- for $\zeta \equiv L^2/4D_0\hat{\tau} \gg 1$ (the extension of electron sphere $\lambda \equiv \sqrt{4D_0\hat{\tau}}$ is small)

$$\mathcal{G}^{1D}(z, \hat{\tau}) = \sum_{n=-\infty}^{\infty} (-1)^n \frac{\theta(\hat{\tau})}{\sqrt{4\pi D_0\hat{\tau}}} \exp\left(-\frac{z_n^2}{4D_0\hat{\tau}}\right), \quad (8)$$

where $z_n = 2Ln + (-1)^n z$;

- otherwise

$$\mathcal{G}^{1D}(z, \hat{\tau}) = \frac{1}{L} \sum_{n=1}^{\infty} [\exp(-D_0 k_n'^2 \hat{\tau}) \phi_n'(0) \phi_n'(z)], \quad (9)$$

where

$$\phi_n(z) = \sin[k_n(L - |z|)]; \quad k_n = (n - 1/2)\pi/L, \quad (10)$$

$$\phi_n'(z) = \sin[k_n'(L - z)]; \quad k_n' = n\pi/L. \quad (11)$$

For any source function $q(r, z, \theta; E_S)$ the local observed flux of positrons can be written as

$$\Phi_{\odot} = \frac{v}{4\pi} \times 2 \int_0^L dz \int_0^{R_{\max}} r dr \int_E^{\infty} dE_S \mathcal{G}_{\odot}(r, z, E \leftarrow E_S) \int_0^{2\pi} d\theta q(r, z, \theta; E_S). \quad (12)$$

For the propagation parameters, we use the medium (referred as ‘‘MED’’) set of parameters which is derived through fitting the observational B/C data given in Ref. [27], i.e., $D_0 = 0.0112 \text{ kpc}^2 \text{ Myr}^{-1}$, $\delta = 0.70$ and the height of the diffusive halo $L = 4 \text{ kpc}$.

III. GAMMA RAYS

For the purely leptonic annihilation or decay of DM particles, γ -rays can be generally produced in two ways. One is the final state radiation (FSR) which is emitted directly from the external legs when DM particles annihilates or decays to charged leptons³. The other is the IC scattering photons from ISRF when the electrons and positrons propagate in the MW. Compared with the IC photons, the FSR has several advantages. First the spectrum of FSR is unique and may give smoking gun diagnostic for DM signal. In addition, the FSR does not depend on the astrophysical environment such as the distribution of ISRF. Therefore in this work we only consider the FSR. It will simplify the calculation, meanwhile the results obtained on the constraints on the model parameters is also conservative.

³ Note that for the tau channel, the decay of τ leptons will produce a large number of neutral pions which can then decay into photons. We also include this contribution in the FSR.

The photon yield spectrum for e^\pm or μ^\pm channel for $m_\chi \gg m_e, m_\mu$ can be written as [28, 29]

$$\left. \frac{dN}{dx} \right|_i = \frac{\alpha}{\pi} \frac{1 + (1-x)^2}{x} \log \left(\frac{s}{m_i^2} (1-x) \right), \quad (13)$$

where $\alpha \approx 1/137$ is the fine structure constant, $i = e, \mu$. For DM annihilation we have $s = 4m_\chi^2$ and $x = E_\gamma/m_\chi$; while for DM decay $s = m_\chi^2$ and $x = 2E_\gamma/m_\chi$ [30]. For τ^\pm channel, we adopt the total parameterization including the direct FSR component as shown in Eq.(13) and the decay products from the chain $\tau \rightarrow \pi^0 \rightarrow \gamma$ [31]

$$\left. \frac{dN}{dx} \right|_\tau = x^{-1.31} (6.94x - 4.93x^2 - 0.51x^3) e^{-4.53x}, \quad (14)$$

with the same definition of x as above.

The γ -ray flux along a specific direction can be written as

$$\begin{aligned} \phi(E_\gamma, \psi) &= C \times W(E_\gamma) \times J(\psi) \\ &= \begin{cases} \frac{\rho_\odot^2 R_\odot}{4\pi} \times \frac{\langle \sigma v \rangle}{2m_\chi^2} \frac{dN}{dE_\gamma} \times \frac{1}{\rho_\odot^2 R_\odot} \int_{LOS} \rho^2(l) dl, & \text{for annihilation} \\ \frac{\rho_\odot R_\odot}{4\pi} \times \frac{1}{m_\chi \tau} \frac{dN}{dE_\gamma} \times \frac{1}{\rho_\odot R_\odot} \int_{LOS} \rho(l) dl, & \text{for decay} \end{cases} \end{aligned} \quad (15)$$

where the integral is taken along the line-of-sight (LOS), $W(E)$ and $J(\psi)$ represent the particle physics factor and the astrophysical factor respectively, $R_\odot = 8.5$ kpc is the solar system location from GC, and ρ_\odot is the local DM density. For the emission from a diffuse region with solid angle $\Delta\Omega$, we define the average astrophysical factor as

$$J_{\Delta\Omega} = \frac{1}{\Delta\Omega} \int_{\Delta\Omega} J(\psi) d\Omega, \quad (16)$$

which is fully determined by the parameter γ in Eq.(3).

In this work we use the diffuse γ -ray observation in the sky region $|l| < 0.8^\circ$ and $|b| < 0.3^\circ$ around the GC by H.E.S.S. [21] to constrain the central profile of DM density distribution. It should be noted that the H.E.S.S. observation of the GC ridge γ -ray flux is a background subtracted one. In Ref. [21] the emission from $0.8^\circ < |b| < 1.5^\circ$, $|l| < 0.8^\circ$ is taken as the background. Therefore the H.E.S.S. reported result is not the total emission of the selected sky region, but a lowered one. To compare the calculated result with the data, we calculate the γ -ray flux from DM in the H.E.S.S. signal region ($|b| < 0.3^\circ$, $|l| < 0.8^\circ$) with subtracting the one in the H.E.S.S. background region ($0.8^\circ < |b| < 1.5^\circ$, $|l| < 0.8^\circ$). Thus the $J_{\Delta\Omega}$ factor adopted for the γ -ray calculation actually means $J_{\Delta\Omega}^{\text{sig}} - J_{\Delta\Omega}^{\text{bkg}}$ in the following.

Similar to Ref. [32], we employ a power-law component $\phi = a_\gamma E_\gamma^{-b_\gamma}$ to represent the astrophysical background contribution to the γ -rays. The FSR from DM is then added to the background to fit the observational data. The fit to the γ -ray data is also included in the MCMC code so that we can derive a consistent constraint on the DM density profile.

IV. MCMC METHOD AND RESULTS

A. Method

In our study, we perform a global analysis employing the MCMC technique to determine the parameters related to DM models. The MCMC sampler is implemented by using the Metropolis-Hastings algorithm. It is an efficient procedure for generating samples which lies in the fact that its equilibrium distribution corresponds to the likelihood function in parameter space. Comparing with a traditional approach where the likelihood function is evaluated on a grid of points in parameter space, the MCMC method has the great potential in expanding the dimension of the parameter series, since the computational requirements of MCMC procedures are insensitive to the dimensionality of the parameter space.

Fixing the e^+e^- background, we have the following parameter space:

$$\mathbf{P} \equiv (m_\chi, \langle\sigma v\rangle \text{ or } \tau, B_e, B_\mu, B_\tau, \gamma, a_\gamma, b_\gamma), \quad (17)$$

where m_χ is the DM particle mass, $\langle\sigma v\rangle$ is the annihilation cross section, for decaying DM τ denotes the lifetime, B_e , B_μ and B_τ are the annihilation (or decay) branching ratios of DM particle into e^+e^- , $\mu^+\mu^-$ and $\tau^+\tau^-$ pairs. For the scenario considered in this work, we have the constraint condition $B_e + B_\mu + B_\tau \equiv 1$. The parameter γ parametrizes the DM density profile and a_γ , b_γ are parameters characterizing astrophysical γ -ray background. So in our global fitting procedure 7 free parameters are in general involved.

With variables in (17) we can calculate the theoretical expectations of electrons and positrons produced from DM. However, to compare with the observational data, we still need to give the astrophysical background contribution to the electrons and positrons. Since the background calculation, especially for positrons, is quite complicated and consumes a lot of time, we employ two approaches of the background. Firstly we fix the background calculated by GALPROP package [33] based on a conventional diffusion + convection (DC)

model [12, 34]. It is shown that the conventional GALPROP model can give fairly good description to the CR data before PAMELA/ATIC/Fermi-LAT/H.E.S.S. [12], as well as the all-sky diffuse γ -ray data from EGRET (except the “GeV excess”, [35]) and Fermi-LAT at intermediate latitudes [36]. The GALPROP model parameters are the same as Ref. [12] except for the high energy electron injection spectrum we adopt a slightly softer one 2.58. For the second approach we include a more complete treatment on this problem. A power law function $q_{e^-} = a_{e^-} E_{e^-}^{-b_{e^-}}$ with two free parameters a_{e^-} , b_{e^-} is involved to describe the injection source of primary electrons. For background positrons which are thought to be produced through CRs interact with ISM, we use the locally measured proton and Helium spectra as parameterized in Ref. [10] and an average ISM density $\sim 1 \text{ cm}^{-3}$ to calculate the positron production rate. For the secondaries production from $p - p$ inelastic collision we use the parameterization given in Ref. [37]. The interaction is restricted in a thin disk with half height $\sim 0.1 \text{ kpc}$. The spatial distribution of positron source is neglected, which is demonstrated not to affect the final positron spectrum [24]. In addition, we employ a free factor c_{e^+} lies between 0.5 and 2 to describe the possible uncertainties about the ISM density and the disk height. That is to say, totally we will have 10 free parameters in this approach.

B. Data sets

Since the electron spectrum measurements between ATIC and Fermi-LAT/H.E.S.S. still have discrepancy, for an unbiased study at the current stage we will try to fit two different data sets respectively. One is to combine the PAMELA positron fraction data, ATIC electron data⁴ and the H.E.S.S. γ -ray data (Data set I), and the other is the combination of PAMELA, Fermi-LAT, H.E.S.S. electron and H.E.S.S. γ -ray data (Data set II). Note that for PAMELA we use only the data with energies higher than $\sim 5 \text{ GeV}$ in the MCMC fitting code. The low energy data are thought to be more easily to be affected by the solar modulation. We get the χ^2 by comparing the spectrum between the theoretical expectations

⁴ The ATIC data include ATIC1+ATIC2+ATIC4, which are taken from the talk by J. Isbert in *TANGO in PARIS* workshop, see <http://irfu.cea.fr/Meetings/tangoinparis/main.htm>. From the numerical calculation, we find that the fitting results between ATIC1+ATIC2+ATIC4 and the published ATIC1+ATIC2 data are very similar, but the former one converges much faster and better.

and the corresponding observational values. For the PAMELA, the observation quantity is the positron fraction $e^+/(e^+ + e^-)$, while for ATIC, Fermi-LAT and H.E.S.S. the undistinguished fluxes of positrons and electrons are concerned. We have taken the total likelihood to be the products of the separate likelihoods \mathcal{L} of all the data. In other words, defining $\chi_i^2 \equiv -2 \log \mathcal{L}_i$, we get

$$\chi_{\text{total}}^2 = \sum_i \chi_i^2, \quad (18)$$

where i labels different observational data.

C. Numerical Results

1. Fixed e^+e^- background

Firstly we consider the fixed background approach. The one dimensional probability distributions of the fitting parameters for annihilation DM scenario are shown in Fig.1. The *left* eight panels are for Data set I, and the *right* eight panels are for Data set II respectively. To get the 1D probability of each parameter we have marginalized over the other parameters. The details about the parameters are compiled in Table I.

To reproduce the peak of ATIC observation of Data set I, the mass of DM is found to be ~ 0.70 TeV with annihilation channel almost purely to e^+e^- . The 2σ upper limits for $\mu^+\mu^-$ and $\tau^+\tau^-$ channels are $B_\mu < 0.269$ and $B_\tau < 0.226$ respectively. While for the fit to Data set II, a larger mass $m_\chi \approx 2.2$ TeV with larger B_μ and B_τ which can give softer electron/positron spectra is favored. The e^+e^- channel which can give strongly peaked electron/positron spectra is remarkably suppressed. The 2σ upper limit for B_e is ~ 0.03 .

An important issue is the constraint from GC diffuse γ -rays observed by H.E.S.S.. A strong constraint on the central DM density profile is shown. At 2σ level, we find $\gamma < 0.539$ for Data set I and < 0.515 for Data set II. It is significantly flatter than the canonical NFW profile with $\gamma = 1$ [41]. This indicates that DM particle might not be so cold, but behaves like warm DM instead [32, 42]. We can also note that the probability distributions of B_μ and B_τ are relatively broad for the Data set II fit. The reason for this is due to the degeneracy between $\mu^+\mu^-$ and $\tau^+\tau^-$ channels. We will discuss this issue later.

The results for decaying DM model are shown in Fig. 2 and Table II respectively. We can see that the results are very similar to the annihilation case except for the constraint on the

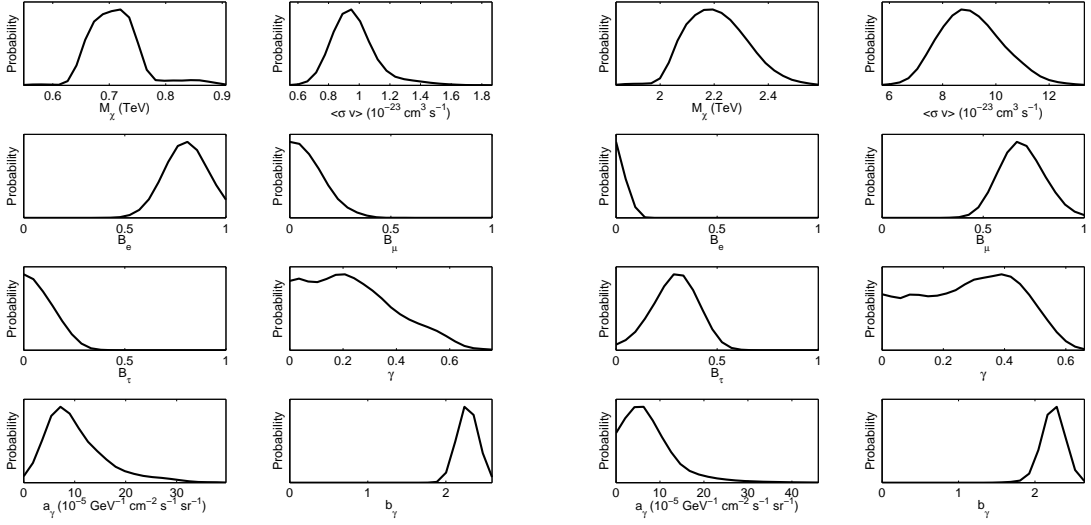


FIG. 1: Probability distributions of the eight parameters in annihilation DM scenario used to fit Data set I (*left*) and II (*right*) respectively, for fixed e^+e^- approach. To get the 1D probability of each parameter we have marginalized over the other parameters.

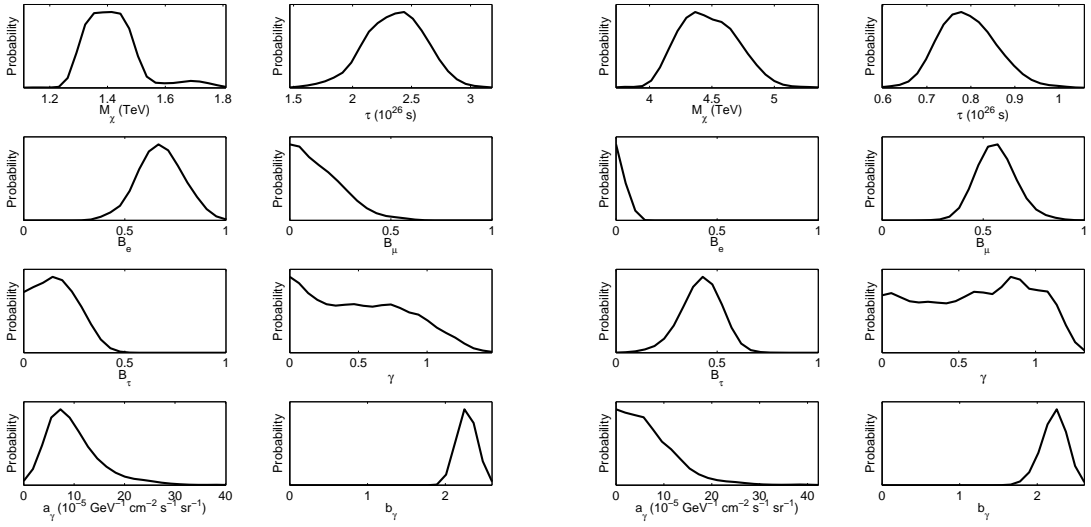


FIG. 2: The same as Fig.1 but for decaying DM scenario.

density profile parameter γ . It is just as expected that since the electron/positron source function is proportional to ρ for DM decay instead of the ρ^2 dependence of DM annihilation,

TABLE I: Mean 1σ errors or 95% limits for the parameters in annihilation DM scenario for the fixed e^+e^- background approach.

Parameters	Data Set I	Data Set II
m_χ (TeV)	$0.711^{+0.032}_{-0.042}$	$2.211^{+0.112}_{-0.111}$
$\langle\sigma v\rangle$ (10^{-23} cm ³ s ⁻¹)	$0.969^{+0.115}_{-0.129}$	$9.105^{+1.177}_{-1.172}$
B_e	0.795 ± 0.090	< 0.031
B_μ	< 0.269	$0.691^{+0.043}_{-0.050}$
B_τ	< 0.226	$0.293^{+0.050}_{-0.044}$
γ	< 0.539	< 0.527
a_γ (10^{-5} GeV ⁻¹ cm ⁻² s ⁻¹ sr ⁻¹)	$10.441^{1.197}_{-3.479}$	< 19.608
b_γ	$2.279^{+0.031}_{-0.033}$	$2.236^{+0.048}_{-0.035}$

TABLE II: Mean 1σ errors or 95% limits for the parameters in decaying DM scenario for the fixed e^+e^- background approach.

Parameters	Data Set I	Data Set II
m_χ (TeV)	$1.418^{+0.064}_{-0.088}$	$4.475^{+0.231}_{-0.233}$
τ (10^{26} s)	$2.359^{+0.252}_{-0.246}$	$0.794^{+0.066}_{-0.063}$
B_e	$0.675^{+0.049}_{-0.050}$	< 0.025
B_μ	< 0.387	$0.565^{+0.032}_{-0.044}$
B_τ	< 0.333	$0.421^{+0.046}_{-0.033}$
γ	< 1.114	< 1.130
a_γ (10^{-5} GeV ⁻¹ cm ⁻² s ⁻¹ sr ⁻¹)	$9.936^{+1.130}_{-3.102}$	< 18.498
b_γ	$2.275^{+0.030}_{-0.035}$	$2.215^{+0.066}_{-0.033}$

the constraint on the central cusp slope is expected to be much weaker.

In Fig. 3 we show the results of the total electron + positron spectra and positron fraction for the best-fitting parameters, for annihilation DM scenario. The results show a very good agreement with the observational data. The results for decaying DM scenario, which are not shown here, are almost undistinguishable from the annihilation case. Because the final states from DM annihilation and decay are completely the same, the only difference comes from the spatial distribution of DM induced electrons/positrons. While the observed high energy

electrons/positrons should mainly come from the local regions near the Earth where there is no big difference between the ρ^2 distribution for DM annihilation and the ρ distribution for DM decay, therefore the propagated electron/positron spectra are very similar for both.

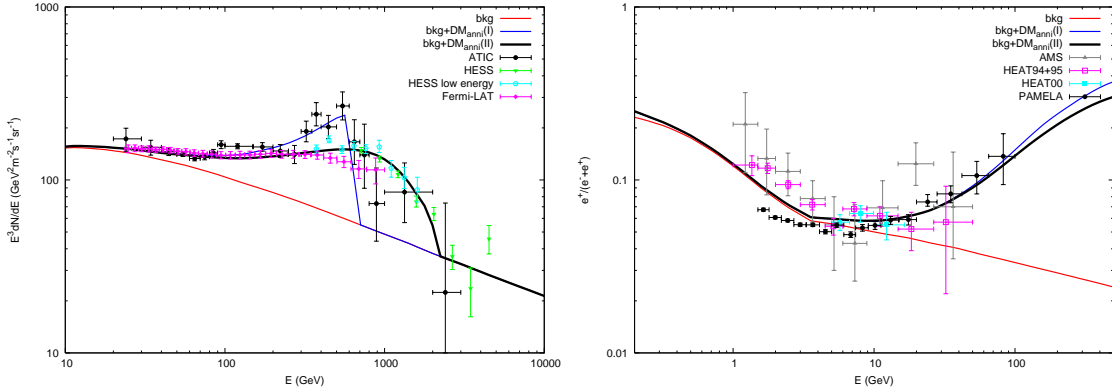


FIG. 3: *Left:* the $e^+ + e^-$ spectrum including the contribution from DM annihilation compared with the observational data from ATIC [2], HESS [4, 5] and Fermi-LAT [6]. *Right:* the $e^+/(e^- + e^+)$ ratio including the contribution from DM annihilation as a function of energy compared with the data from AMS [38], HEAT [39, 40] and PAMELA [1].

Finally we investigate the correlation among the various annihilation or decay channels. We find that there is no evident correlation between parameter B_e and other two branching ratios. This can be understood that the spectrum of electrons/positrons from e^+e^- channel has a very hard and spiky signature, which can be easily distinguished from the other two channels. However, the cases will be different for $\mu^+\mu^-$ and $\tau^+\tau^-$ channels. For the $\mu^+\mu^-$ or $\tau^+\tau^-$ channels, the electrons are generated through the decay of muons or tauons, which both can give a softer electron spectrum. Thus the results from $\mu^+\mu^-$ channel and $\tau^+\tau^-$ channel should have some degeneracies. In Fig. 4 we plot the 2D correlation between B_μ and B_τ for the fit to Data set II, for DM annihilation and decay respectively. It indeed shows a strong anti-correlation between B_μ and B_τ . That means to describe the Data set II the muon channel is equivalent to the tauon channel to some extent. It will be not easy to distinguish whether the DM particle couples mainly with muon flavor or tauon flavor through the electron/positron data. This degeneracy will also lead to an uncertainty on the study of γ -ray prediction or constraint. For tauon channel, more γ -ray photons can be

generated through tauon decay, while for muon channel the FSR radiated γ -ray photons will be much fewer. On the other hand, we expect future accurate γ -ray experiment to break this degeneracy.

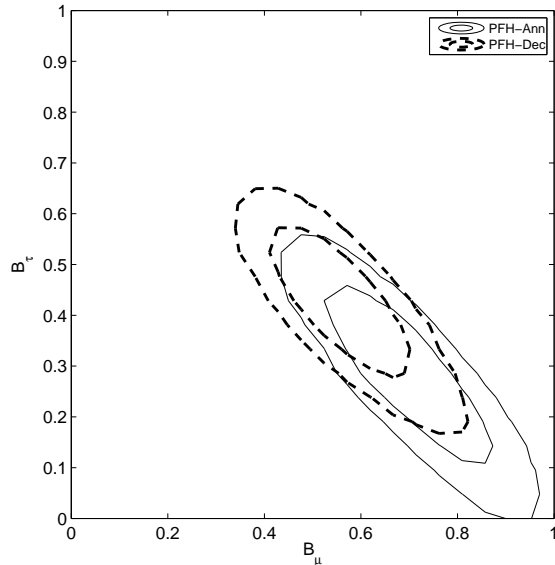


FIG. 4: Two dimensional plot for the correlation between parameters B_μ and B_τ for the fit to Data set II, for DM annihilation (solid) and decay (dashed) respectively. The inner and outer contours show the results at 1σ and 2σ confidence levels.

2. Varying e^+e^- background

In this section, we present the results by setting the e^+e^- background free. Three additional parameters a_{e^-} , b_{e^-} and c_{e^+} are added in the MCMC approach. The $1D$ parameter distributions are shown in Figs. 5, 6 and Tables III, IV respectively, for the four cases as considered in the fixed e^+e^- background section.

We find that there are remarkable effects on the branching ratios if changing the background. This is reasonable since a different background will lead to a different blank for DM to fill. For example if the background electron spectrum is harder, then the required contribution from DM is expected to be softer. Actually if we relax the background electron spectrum, a harder spectrum compared with the previous fixed one is favored according

to the MCMC fit, for both data sets. Thus the branching ratio to $\tau^+\tau^-$ is expected to be larger, while B_e is suppressed. This is extremely evident for Data set I, where $\sim 1/3$ to e^+e^- channel is enough to fit the data and the best-fit B_τ becomes > 0.5 (0.639 for annihilation and 0.655 for decay modes). Since in this case the best-fit background spectrum is about 3.15 after propagation, compared with the one ~ 3.35 of the fixed background, the required electron contribution from DM is much softer. However, a non-negligible branching ratio to e^+e^- is still needed to describe the peak of ATIC data. A combination of $\mu^+\mu^-$ and $\tau^+\tau^-$ is also favored for Data set II, but with $\tau^+\tau^-$ channel dominating instead, compared with the fixed background approach. For other parameters the quantitative constraints are almost unchanged for different background choices.

The changes of the fitting branching ratios between different background choices suggest that we should be cautious when claiming the DM properties used to explain the data, given the uncertain knowledge about the background. While global fitting will be the only way to separate the background and possible ‘‘signal’’, and derive model-independent implications of the data.

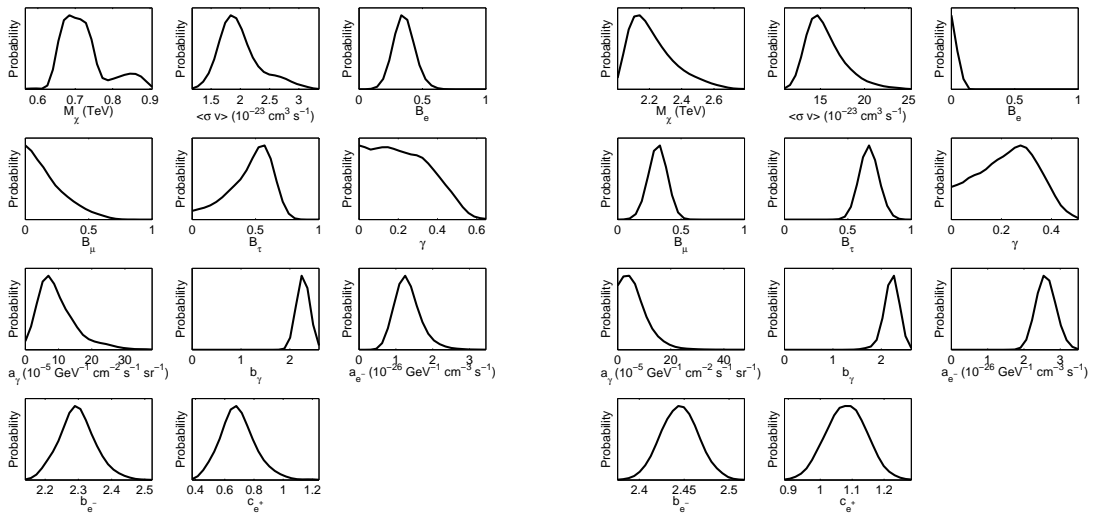


FIG. 5: Probability distributions of the eleven parameters in annihilation DM scenario used to fit Data set I (*left*) and II (*right*) respectively, for varying e^+e^- background approach.

With including additional parameters, we find that the constraints on each parameter are broader comparing with the fixed background approach, however, the goodness of fit defined

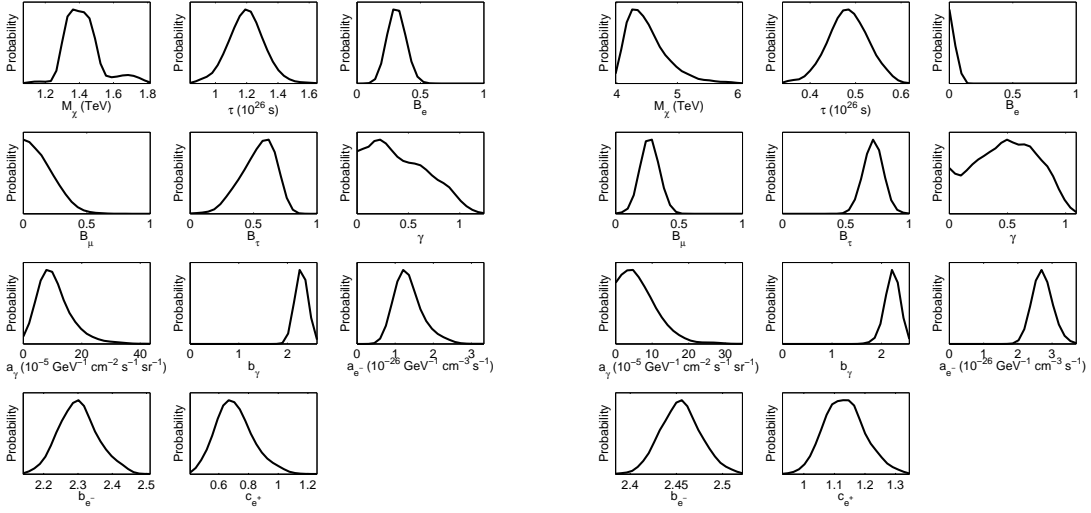


FIG. 6: The same as Fig.5 but for decaying DM scenario.

TABLE III: Mean 1σ errors or 95% limits for the parameters in annihilation DM scenario, for the varying e^+e^- background approach.

Parameters	Data Set I	Data Set II
m_χ (TeV)	$0.723^{+0.063}_{-0.055}$	$2.221^{+0.141}_{-0.184}$
$\langle\sigma v\rangle$ (10^{-23} cm 3 s $^{-1}$)	$1.996^{+0.341}_{-0.311}$	$15.625^{+2.072}_{-1.972}$
B_e	$0.355^{+0.029}_{-0.034}$	< 0.017
B_μ	< 0.486	$0.316^{+0.027}_{-0.025}$
B_τ	$0.459^{+0.099}_{-0.052}$	$0.667^{+0.026}_{-0.029}$
γ	< 0.472	< 0.402
a_γ (10^{-5} GeV $^{-1}$ cm $^{-2}$ s $^{-1}$ sr $^{-1}$)	$9.793^{+1.264}_{-3.328}$	< 16.565
b_γ	$2.270^{+0.036}_{-0.034}$	$2.211^{+0.057}_{-0.033}$
a_e^- (10^{-26} GeV $^{-1}$ cm $^{-3}$ s $^{-1}$)	$1.330^{+0.095}_{-0.176}$	$2.609^{+0.101}_{-0.116}$
b_e^-	$2.297^{+0.052}_{-0.053}$	2.445 ± 0.020
c_e^+	$0.691^{+0.112}_{-0.111}$	1.082 ± 0.063

as $G.O.F = \chi^2/d.o.f$ is getting better (Tab V).

TABLE IV: Mean 1σ errors or 95% limits for the parameters in decaying DM scenario for the varying e^+e^- background approach.

Parameters	Data Set I	Data Set II
m_χ (TeV)	$1.420^{+0.067}_{-0.094}$	$4.501^{+0.305}_{-0.308}$
τ (10^{26} s)	$1.198^{+0.107}_{-0.106}$	$0.483^{+0.043}_{-0.042}$
B_e	$0.312^{+0.026}_{-0.030}$	< 0.026
B_μ	< 0.366	$0.269^{+0.027}_{-0.030}$
B_τ	$0.534^{+0.078}_{-0.051}$	$0.715^{+0.031}_{-0.030}$
γ	< 0.917	< 0.893
a_γ (10^{-5} GeV $^{-1}$ cm $^{-2}$ s $^{-1}$ sr $^{-1}$)	$10.924^{+1.306}_{-3.170}$	< 16.377
b_γ	$2.287^{+0.033}_{-0.030}$	$2.216^{+0.057}_{-0.034}$
a_e^- (10^{-26} GeV $^{-1}$ cm $^{-3}$ s $^{-1}$)	$1.352^{+0.093}_{-0.196}$	$2.720^{+0.100}_{-0.129}$
b_e^-	$2.301^{+0.057}_{-0.056}$	2.455 ± 0.021
c_e^+	$0.708^{+0.120}_{-0.117}$	1.134 ± 0.065

TABLE V: The reduced χ_r^2 of each case.

	Fixed		Varying	
	Anni	Decay	Anni	Decay
Data Set I	1.439	1.434	1.065	1.075
Data Set II	1.143	1.151	1.057	1.112

V. SUMMARY

In this work we employ a MCMC technique to determine the parameters of DM scenario in interpreting the recent observations of electron spectra and positron fraction data. Both the DM annihilation and decay are considered in this work. The DM particle is assumed to couple only with leptons. Considering the discrepancy between experimental data from ATIC and Fermi-LAT/H.E.S.S., we fit two data sets independently. We find that for Data set I (PAMELA+ATIC), DM with $m_\chi \approx 0.7$ TeV for annihilation (or 1.4 TeV for decay) and a non-negligible e^+e^- component is favored. For Data set II (PAMELA+Fermi-LAT+H.E.S.S.) $m_\chi \approx 2.2$ TeV for annihilation (or 4.5 TeV for decay) and the combination

of $\mu^+\mu^-$ and $\tau^+\tau^-$ final states can best fit the data. There is degeneracy between parameters B_μ and B_τ . The constraint on the central density profile of DM halo from the diffuse γ -rays near the GC is also included in the MCMC code self-consistently. We find the H.E.S.S. observations of the GC γ -rays can give strong constraint on the DM density slope of the central cusp for the annihilation DM scenario. In that case the NFW profile with $\gamma = 1$, which is regarded as the typical predication from cold DM scenario, is excluded with a high significance ($> 3\sigma$). For the decaying DM scenario, the constraint is much weaker.

We find that the largest uncertainties on the determination of DM branching ratios come from the limited understanding of the e^+e^- background. Besides using the canonical background expectations from CR propagation models, we further consider the approach to involve the background uncertainties. Three additional free parameters are adopted to describe the background contribution and fitted globally with the DM parameters. It is shown that the branching ratios depend sensitively on the background results. The limited knowledge about the background actually prevents us from a precise determination of the DM final state information. However, with the accumulation of more observational data from PAMELA, AMS02 and many other upcoming experiments with much higher precision and detailed information of each species, we may expect to get better understanding on both the background and the “exotic signal” (if exists). While global fitting will be the only way to separate the background and signal, and derive model-independent implications of the data. Since the MCMC method works in a full high-dimensional parameter space, the code developed in this work will be a useful tool in studying both the CR physics and the exotic new physics, given more precise observational data in the future.

We do not include the radio constraints on the synchrotron radiation of the models in this work, though the radio observations in the GC region might set even stronger constraints than γ -rays, as studied in Refs. [43–45]. The radio constraints are found to be sensitive to the DM profile, instead of the central most configuration of the magnetic field. However, since the knowledge of the magnetic field relies on some assumptions such as the accretion state of central black hole and the equipartition of the matter kinetic energy with the magnetic pressure [44], we think there are still uncertainties of the radio constraints. Additionally, one expects that antiproton constraints would be important for the tau channel, which has not yet been considered in the current work. This combined with the radio bound may provide a stringent constraint for the τ channel, which deserves a detailed study in future.

As an end, we would like to mention that, there exists a self-consistent way to explain the current data by introducing a light mediator state in DM annihilation (or decay) [46], which has not yet been considered in the current work. The distinct advantages of this type of models are that, the strongly constrained decay into hadrons is kinematically forbidden, and Sommerfeld enhancement with small velocity of Galactic DM allows for the large annihilation cross sections required by observations. This kind of model is not included in this work due to the fact that, we need to introduce more parameters in the fitting such as the mass of the mediator which can not be effectively constrained by the current data on the one hand, and the present work is the first step of the application of MCMC method in DM indirect searches on the other hand. We hope the forthcoming improvement of the method can partially address this issue.

Acknowledgements

We thank Jun-Qing Xia, Yi-Fu Cai for discussion. This work is supported in part by National Natural Science Foundation of China under Grant Nos. 90303004, 10533010, 10675136 and 10803001 and by the Chinese Academy of Science under Grant No. KJCX3-SYW-N2.

-
- [1] O. Adriani *et al.*, Nature **458**, 607 (2009) [arXiv:0810.4995 [astro-ph]].
 - [2] J. Chang *et al.*, Nature **456** (2008) 362.
 - [3] S. Torii *et al.*, arXiv:0809.0760 [astro-ph].
 - [4] F. Aharonian *et al.*, Phys. Rev. Lett. **101**, 261104 (2008) [arXiv:0811.3894 [astro-ph]].
 - [5] F. Aharonian *et al.*, arXiv:0905.0105 [astro-ph.HE].
 - [6] A. A. Abdo *et al.*, Phys. Rev. Lett. **102**, 181101 (2009) [arXiv:0905.0025 [astro-ph.HE]].
 - [7] L. Bergstrom, arXiv:0903.4849 [hep-ph].
 - [8] X. G. He, Mod. Phys. Lett. A **24**, 2139 (2009) [arXiv:0908.2908 [hep-ph]].
 - [9] O. Adriani *et al.*, Phys. Rev. Lett. **102**, 051101 (2009) [arXiv:0810.4994 [astro-ph]].
 - [10] F. Donato, D. Maurin, P. Brun, T. Delahaye and P. Salati, Phys. Rev. Lett. **102**, 071301 (2009) [arXiv:0810.5292 [astro-ph]].
 - [11] M. Cirelli, M. Kadastik, M. Raidal and A. Strumia, Nucl. Phys. B **813**, 1 (2009)

- [arXiv:0809.2409 [hep-ph]].
- [12] P. F. Yin, Q. Yuan, J. Liu, J. Zhang, X. J. Bi, S. H. Zhu and X. M. Zhang, *Phys. Rev. D* **79**, 023512 (2009) [arXiv:0811.0176 [hep-ph]].
- [13] E. Nardi, F. Sannino and A. Strumia, *JCAP* **0901**, 043 (2009) [arXiv:0811.4153 [hep-ph]].
- [14] I. Cholis, G. Dobler, D. P. Finkbeiner, L. Goodenough and N. Weiner, arXiv:0811.3641 [astro-ph].
- [15] L. Bergstrom, J. Edsjo and G. Zaharijas, arXiv:0905.0333 [astro-ph.HE].
- [16] P. Meade, M. Papucci, A. Strumia and T. Volansky, arXiv:0905.0480 [hep-ph].
- [17] J. Zhang, X. J. Bi, J. Liu, S. M. Liu, P. F. Yin, Q. Yuan and S. H. Zhu, arXiv:0812.0522 [astro-ph].
- [18] D. Gamerman, *Markov Chain Monte Carlo: Stochastic simulation for Bayesian inference* (Chapman and Hall, 1997).
- [19] D. J. C. MacKay (2002), <http://www.inference.phy.cam.ac.uk/mackay/itprnm/book.html>.
- [20] R. M. Neil (1993), <ftp://ftp.cs.utoronto.ca/pub/~radford/review.ps.Z>.
- [21] F. Aharonian *et al.* [H.E.S.S. Collaboration], *Nature* **439**, 695 (2006) [arXiv:astro-ph/0603021].
- [22] X. X. Xue *et al.*, *Astrophys. J.* **684**, 1143 (2008) [arXiv:0801.1232 [astro-ph]].
- [23] J. S. Bullock *et al.*, *Mon. Not. Roy. Astron. Soc.* **321**, 559 (2001).
- [24] T. Delahaye, F. Donato, N. Fornengo, J. Lavalle, R. Lineros, P. Salati and R. Taillet, *Astron. Astrophys.* **501**, 821 (2009) [arXiv:0809.5268 [astro-ph]].
- [25] J. Lavalle, J. Pochon, P. Salati and R. Taillet, *Astron. Astrophys.* **462**, 827 (2007). [arXiv:astro-ph/0603796].
- [26] J. Lavalle, Q. Yuan, D. Maurin and X. J. Bi, *Astron. Astrophys.* **479**, 427 (2008) [arXiv:0709.3634 [astro-ph]].
- [27] F. Donato, N. Fornengo, D. Maurin, P. Salati and R. Taillet, *Phys. Rev. D* **69**, 063501 (2004) [arXiv:astro-ph/0306207].
- [28] L. Bergstrom, T. Bringmann, M. Eriksson and M. Gustafsson, *Phys. Rev. Lett.* **94**, 131301 (2005) [arXiv:astro-ph/0410359].
- [29] J. F. Beacom, N. F. Bell and G. Bertone, *Phys. Rev. Lett.* **94**, 171301 (2005) [arXiv:astro-ph/0409403].
- [30] R. Essig, N. Sehgal and L. E. Strigari, arXiv:0902.4750 [hep-ph].
- [31] N. Fornengo, L. Pieri and S. Scopel, *Phys. Rev. D* **70**, 103529 (2004) [arXiv:hep-ph/0407342].

- [32] X. J. Bi, R. Brandenberger, P. Gondolo, T. Li, Q. Yuan and X. Zhang, arXiv:0905.1253 [hep-ph].
- [33] A. W. Strong and I. V. Moskalenko, *Astrophys. J.* **509**, 212 (1998). [arXiv:astro-ph/9807150]; I. V. Moskalenko and A. W. Strong, *Astrophys. J.* **493**, 694 (1998). [arXiv:astro-ph/9710124]. <http://galprop.stanford.edu/>
- [34] A. M. Lionetto, A. Morselli and V. Zdravkovic, *JCAP* **0509**, 010 (2005). [arXiv:astro-ph/0502406].
- [35] A. W. Strong, I. V. Moskalenko and O. Reimer, *Astrophys. J.* **537**, 763 (2000) [Erratum-ibid. **541**, 1109 (2000)] [arXiv:astro-ph/9811296].
- [36] A. A. Abdo, *Astrophys. J.* **703**, 1249 (2009) [arXiv:0908.1171 [astro-ph.HE]].
- [37] T. Kamae, N. Karlsson, T. Mizuno, T. Abe and T. Koi, *Astrophys. J.* **647**, 692 (2006) [Erratum-ibid. **662**, 779 (2007)] [arXiv:astro-ph/0605581].
- [38] M. Aguilar *et al.* [AMS-01 Collaboration], *Phys. Lett. B* **646**, 145 (2007) [arXiv:astro-ph/0703154].
- [39] S. W. Barwick *et al.* [HEAT Collaboration], *Astrophys. J.* **482**, L191 (1997) [arXiv:astro-ph/9703192].
- [40] S. Coutu *et al.*, *Proc. 27th Int. Cosmic Ray Conf.* **5**, 1687 (2001).
- [41] J. F. Navarro, C. S. Frenk and S. D. M. White, *Astrophys. J.* **490**, 493 (1997).
- [42] W. B. Lin, D. H. Huang, X. Zhang and R. H. Brandenberger, *Phys. Rev. Lett.* **86**, 954 (2001) [arXiv:astro-ph/0009003].
- [43] M. Regis and P. Ullio, *Phys. Rev. D* **78**, 043505 (2008) [arXiv:0802.0234 [hep-ph]].
- [44] G. Bertone, M. Cirelli, A. Strumia and M. Taoso, *JCAP* **0903**, 009 (2009) [arXiv:0811.3744 [astro-ph]].
- [45] L. Bergstrom, G. Bertone, T. Bringmann, J. Edsjo and M. Taoso, *Phys. Rev. D* **79**, 081303 (2009) [arXiv:0812.3895 [astro-ph]].
- [46] N. Arkani-Hamed, D. P. Finkbeiner, T. R. Slatyer and N. Weiner, *Phys. Rev. D* **79**, 015014 (2009) [arXiv:0810.0713 [hep-ph]].